Highly Sensitive and Wearable In_2O_3 Nanoribbon Transistor Biosensors with Integrated On-Chip Gate for Glucose Monitoring in Body Fluids

Qingzhou Liu, [1] Yihang Liu, [2] Fanqi Wu, [1] Xuan Cao, [1] Zhen Li,[2] Mervat Alharbi, [3] Ahmad N. Abbas, [4,5] Moh R. Amer, [*3,6] and Chongwu Zhou[*1, 2]

[1] Mork Family Department of Chemical Engineering and Materials Science and [2] Ming Hsieh Department of Electrical Engineering, University of Southern California, Los Angeles, California 90089, United States.

[3] Center of Excellence for Green Nanotechnologies, Joint Centers of Excellence Program, King Abdulaziz City for Science and Technology, P.O Box 6086, Riyadh 11442, Saudi Arabia.

[4] Department of Electrical and Computer Engineering, University of Jeddah, 285 Dhahban 23881, Saudi Arabia

[5] Department of Electrical and Computer Engineering, King Abdulaziz University, Abdullah Sulayman Street, Jeddah, 22254, Saudi Arabia

[6] Department of Electrical Engineering, 420 Westwood Plaza, 5412 Boelter Hall, University of California, Los Angeles, Los Angeles, California 90095, United States.

* To whom correspondence should be addressed. E-mail: mamer@seas.ucla.edu and chongwuz@usc.edu.

S1. AFM and XRD characterization of In_2O_3 nanoribbons

To characterize the In_2O_3 nanoribbons, we used atomic force microscopy (AFM) and X-ray diffraction (XRD) on samples deposited on PET substrate (Figure S1). The AFM images (Figure S1a and Figure S1b) show that the nanoribbons are solid and have clear edges. The height profile (Figure S1a inset) shows the thickness of In_2O_3 nanoribbons is ~ 20 nm. The XRD pattern shown in Figure S1c presents only PET peaks, indicating the In_2O_3 is amorphous.

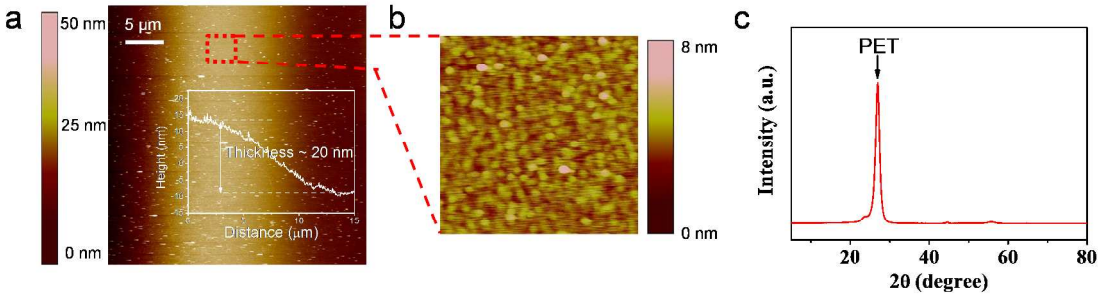

Figure S1. (a) AFM image with height profile of a ~ 20 nm thick In_2O_3 nanoribbon. (b) Zoom-in AFM scan of a 1 μm × 1 μm square on the In_2O_3 film. (c) XRD of RF sputtered In_2O_3 film deposited on top of PET substrate.

S2. Mobility calculation

The field-effect mobility of the In_2O_3 FET is calculated using the following equation:

$$g_m = \frac{dI_D}{dV_{GS}} = \frac{W}{L} C_{DL} \mu_{FE} V_D \quad (1)$$

Where W is the channel width, L is the channel length, and C_{DL} is the electrical double layer capacitance per unit area in 0.1 M ionic strength aqueous solution reported previously (25.52 μF cm^{-2}).[2] The maximum transconductance 5.69 μS was obtain at a drain voltage of 0.2 V and gate voltage of 0.527 V as shown in Figure S2.

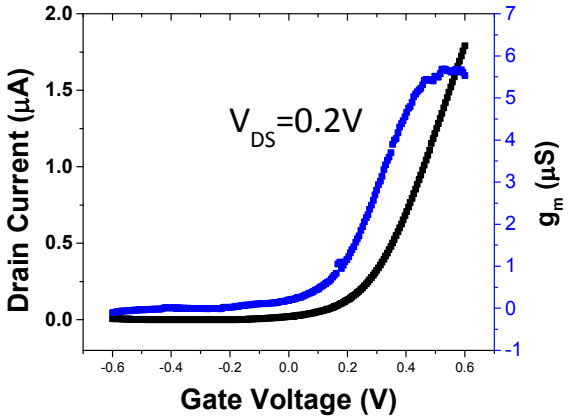

Figure S2. A representative transfer curve of an In_2O_3 nanoribbon FET with V_{DS} = 0.2 V and its g_m.

S3. Statistical study

We also conducted a statistical study of key electrical properties for 50 In_2O_3 nanoribbon devices on a biosensor chip measured in 0.1 x PBS and biased through the Ag/AgCl electrode and the gold side gate. Figure S2 shows that the device performance including mobility (μ), threshold voltage (V_{th}), on/off ration and on-state current, is very similar when using gold side gate electrodes and Ag/AgCl gate electrodes.

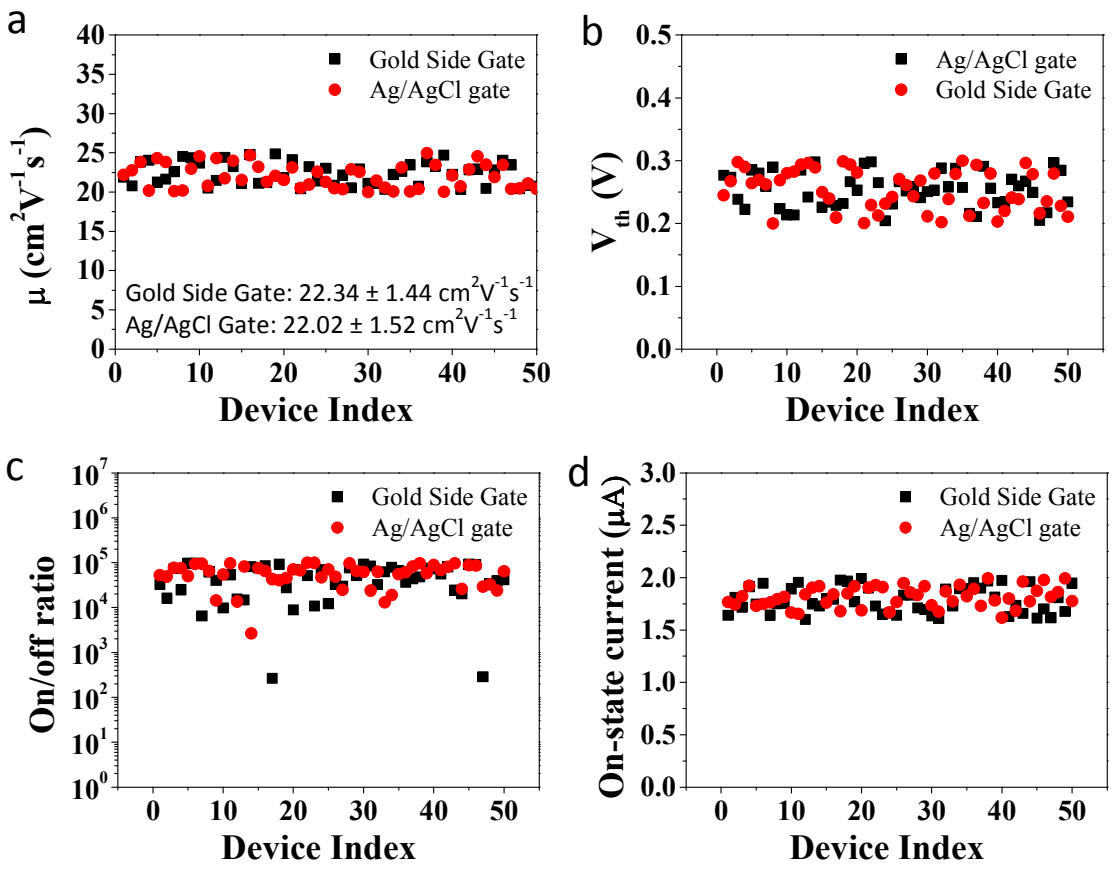

Figure S3. Electrical performance of 50 In_2O_3 nanoribbon transistors (a) Mobilities (μ), (b) Threshold voltage (V_{TH}), (c) On/off current ratios at V_{DS} = 0.2 V, and (d) On-state current (I_{ON}) at V_{GS} = 0.6 V and V_{DS} = 0.2 V.

S4. Bending test

In order to characterize the flexibility of the wearable In_2O_3 FETs, bending tests were carried out on both functionalized and unfunctionalized devices. We tightly wrapped our fabricated In_2O_3 foil around cylinder with different radius of curvatures. The electrical performance of the devices under tensile strain was measured in aqueous environment. In Figure S3, we compared transfer curves of a representative In_2O_3 biosensor FET under different bending radius and with different bending cycles.

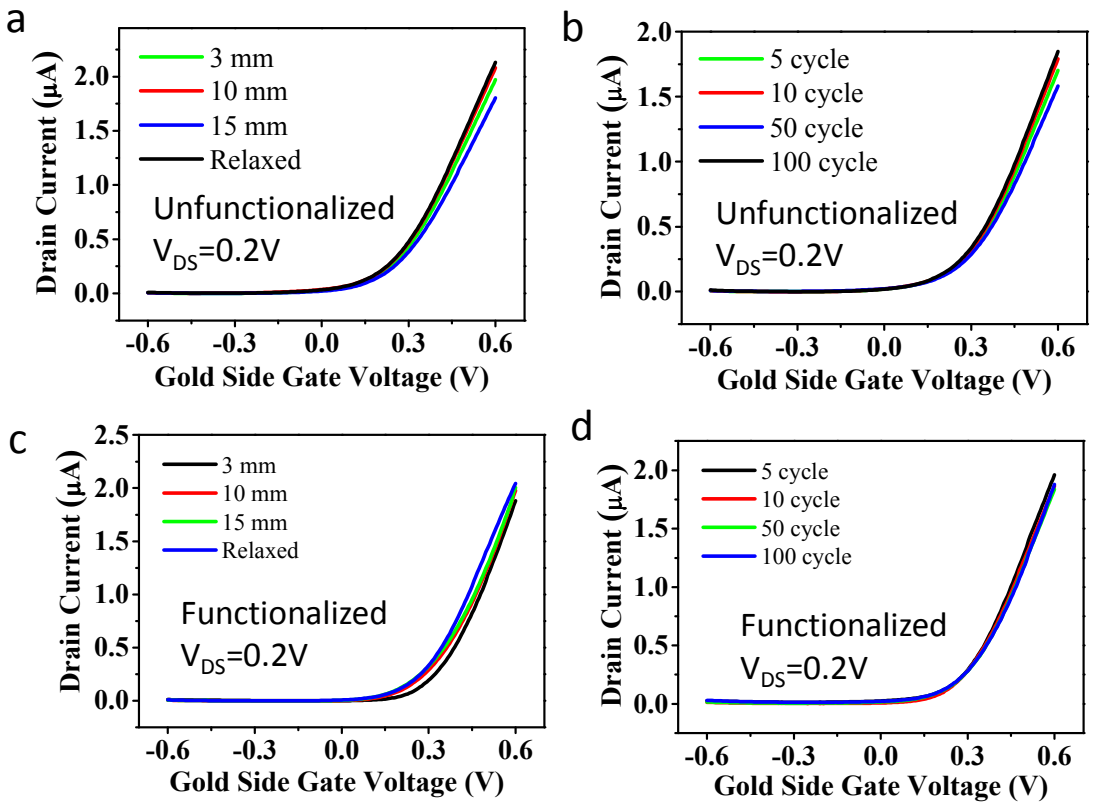

Figure S4. Transfer characteristics of (a) an unfunctionalized In_2O_3 FET under relaxed state, bent with a radius of ~3, 10, and 15 mm, (b) an unfunctionalized In_2O_3 FET after bending with 5, 10, 50, and 100 cycles, (c) a functionalized In_2O_3 FET under relaxed state, bent with a radius of ~3, 10, and 15 mm, and (d) a functionalized In_2O_3 FET after bending with 5, 10, 50, and 100 cycles.

S5. Tensile strain calculation

To calculate the tensile strain when the wearable In_2O_3 nanoribbon FET foil was wrapped tightly around a cylinder with radius ~ 3 mm, we used the following formula[1]:

$$\varepsilon = \frac{1}{R} \times \frac{d_s + d_f}{2} \times \frac{\chi \cdot \gamma^2 + 2 \cdot \chi \cdot \gamma + 1}{\chi \cdot \gamma^2 + \chi \cdot \gamma + \gamma + 1}$$

Here, R is the bending radius, d_s is the thickness of the substrate, and d_f is the thickness of In_2O_3 nanoribbon transistor (TFT). $\gamma = d_f / d_s$ and $\chi = Y_f / Y_s$, where Y_f and Y_s are the Young's modulus of In_2O_3 FET and the substrate, respectively. We assume $Y_f = Y_s$ and the above equation can be further simplified:

$$\varepsilon = \frac{1}{R} \times \frac{d_s + d_f}{2}$$

The thickness of the substrate is 15 μm and the total thickness of the TFT is less than 100 nm. With the bending radius of 3 mm, the tensile strain is calculated to be ~ 0.25%. We have further plotted out the mobility as a function of tensile strain.

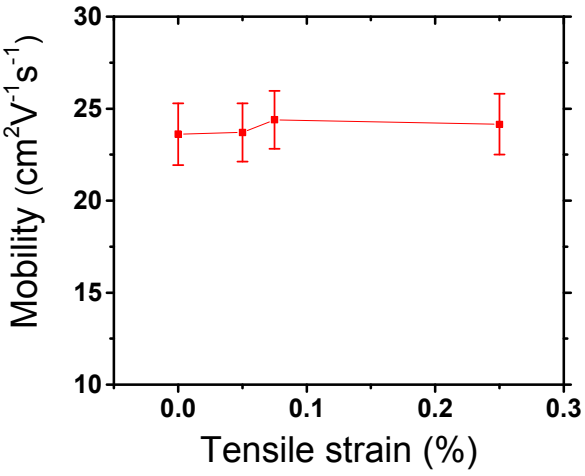

Figure S5. The mobilities of In_2O_3 FETs as a function of tensile strain.

S6. PH sensing

To further confirm the sensing ability of our biosensor platform, we conducted pH sensing experiments to test the ionic sensitivity of the biosensor chip in responses to commercial pH solutions. Figure S4 shows the real-time sensing response of an In_2O_3 FET to standard pH calibration solutions. The initial current I_o was obtained by using PBS to stabilize the device, and then the PBS buffer was sequentially changed to commercial pH buffer solutions ranging from pH 10 to pH 5. The drain current responded quickly and log-linearly to each pH buffer.

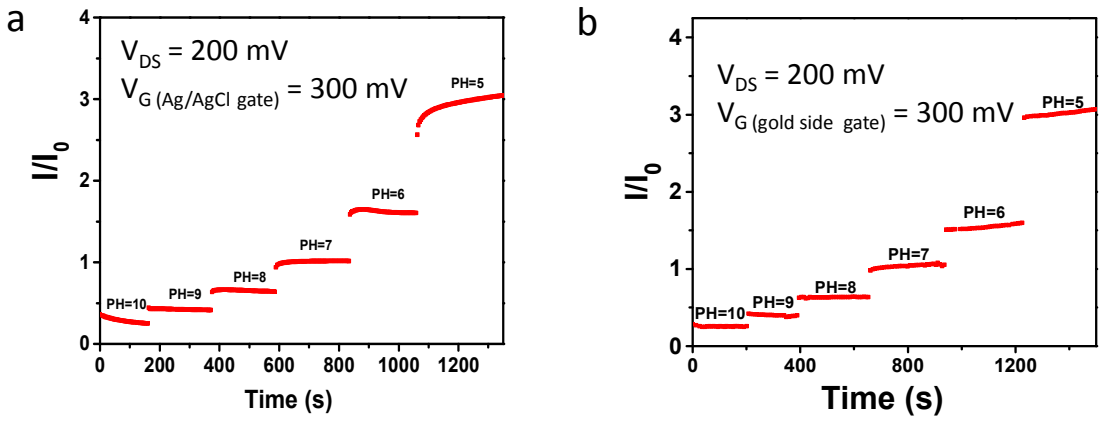

Figure S6. Real-time sensing responses of an In_2O_3 FET to standard pH calibration solutions. Gate voltage is applied with (a) a Ag/AgCl gate electrode, and (b) a gold side gate electrode.

S7. Glucose sensing control experiment

To further confirm that the environment changes are introduced by the reaction of glucose and glucose oxidase, we performed a control experiment on sensors without glucose oxidase. In this control experiment, we functionalized the surface of the gold electrodes with chitosan and carbon nanotube only. We sequentially added glucose in 0.1 x PBS with concentrations of 1 μM, 10 μM, 100 μM, and 1 mM. As expected, sensors did not respond to glucose as shown in Figure S5.

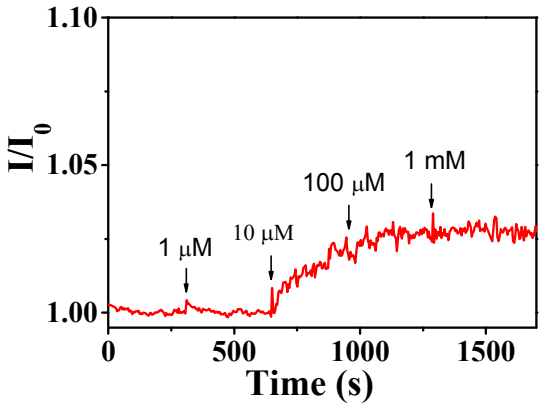

Figure S7. Glucose sensing results of an In_2O_3 nanoribbon biosensor functionalized with chitosan and SWCNT only.

S8. Stability tests of glucose sensors

We characterized an In_2O_3 biosensor with functionalization (chitosan/CNT/GOx) for 2 weeks. The device was measured every day and store at 4 □ after each measurement. The sensing signals shows very small differences in first 4 days and the responses to 10 μM and 100 μM glucose in PBS decreased for about 25% and 30% after 2 weeks, respectively (Figure S7 in the Supporting Information). The decrease of the sensing responses can be attributed to the deactivation of the enzyme glucose oxidase over a long time, and the loss of the enzymes during washing steps. The degradation of the devices will not be a problem in consideration of our low-cost disposable biosensors.

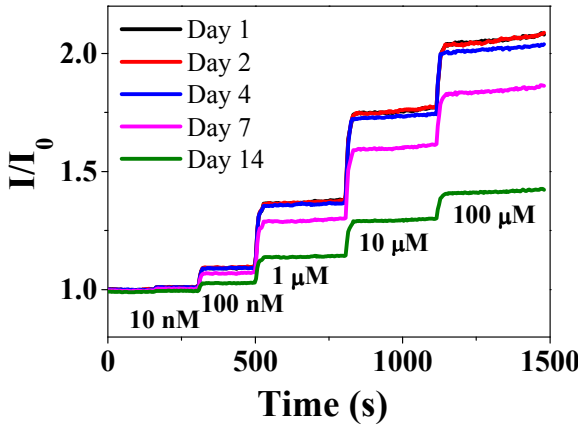

Figure S8. Glucose sensing results with a functionalized sensor after 1, 2, 4, 7, and 14 days.

Reference:

1. Cao, X.; Cao, Y.; Zhou, C., Imperceptible and Ultraflexible p-Type Transistors and Macroelectronics Based on Carbon Nanotubes. *ACS Nano* **2016**, 10, 199-206.
2. Park, S.; Lee, S.; Kim, C.-H.; Lee, I.; Lee, W.-J.; Kim, S.; Lee, B.-G.; Jang, J.-H.; Yoon, M.-H., Sub-0.5 V Highly Stable Aqueous Salt Gated Metal Oxide Electronics. *Sci. Rep.* **2015**, 5, 13088.